

ISO OBSERVATIONS OF FINE-STRUCTURE ATOMIC LINES FROM PROTO-PLANETARY NEBULAE

A. Castro-Carrizo¹, D. Fong², V. Bujarrabal¹, M. Meixner², A.G.G.M. Tielens³, W.B. Latter⁴, and M.J. Barlow⁵

¹Observatorio Astronómico Nacional, Apartado 1143, E-28800 Alcalá de Henares, Spain

²University of Illinois, 1002 W. Green St., Urbana, IL61801, USA

³Kapteyn Astronomical Institute, P.O. Box 800, 9700 AV Groningen, The Netherlands

⁴SIRTF Science Center/IPAC, CalTech, MS 314-6, Pasadena, CA 91125, USA

⁵Department of Physics and Astronomy, University College London, Gower Street, London WC1E 6BT, United Kingdom

ABSTRACT

We present ISO observations of fine-structure atomic lines from 24 evolved sources. Most of them are proto-planetary nebulae (PPNe) but we also include a few AGB stars and planetary nebulae. Data on O⁰, C⁺, N⁺, Si⁰, Si⁺, S⁰, Fe⁰ and Fe⁺ were obtained. PPNe are found to emit through low-excitation atomic lines only when the central star is hotter than ~ 10000 K. This result suggests that such lines predominantly arise from Photo-Dissociation Regions (PDRs). Our results are also in reasonable agreement with predictions from PDR emission models, allowing the estimation of the density of the emitting layers from comparison with the model parameters. However, Fabry-Perot ISO observations suggest in some cases a contribution from shocked regions, in spite of their poor sensitivity and spectral resolution. The intensity of the [C II] 158 μm line has been used to measure the amount of low-excitation atomic mass in PPNe, since this transition has been found to be a useful model-independent probe to estimate the total mass of this component. In the most evolved sources the atomic mass is very high (up to $\sim 1 M_{\odot}$), representing in some cases the dominant nebular component.

Key words: Atomic data – Stars: AGB and post-AGB – (*Stars:*) circumstellar matter – Stars: mass-loss – (*ISM:*) planetary nebulae

1. INTRODUCTION

In the last phases of the life of low mass stars ($< 8 M_{\odot}$), a fast evolution from the Asymptotic Giant Branch (AGB) to planetary nebulae (PNe) takes place. AGB stars lose most of their mass, forming a cool molecular envelope that expands isotropically at low velocity ($\sim 15 \text{ km s}^{-1}$). In less than 1000 years these cool and extended AGB stars, and their respective molecular envelopes, evolve becoming a tiny and very hot blue dwarf surrounded by a mostly ionized nebula. In the intermediate stage, the proto-planetary nebulae (PPNe) often show intermediate chemical and physical properties between those of AGB envelopes and PNe. At some point of this evolution the post-AGB star

ejects a very fast and collimated wind that collides with the remnant of the AGB envelope. This phenomenon is thought to determine the morphology and dynamics of the PPN.

Both the increase of the temperature of the central star and the presence of shocks can originate the dissociation of the molecules in the envelope. The photodissociation regions (PDRs), that were theoretically studied by Tielens & Hollenbach (1985), are mainly cooled through fine-structure atomic lines, the heating being due to the far-ultraviolet photons absorbed by the dust grains. Those lines are excited collisionally at temperatures of $\sim 10^2$ - 10^3 K. On the other hand, the presence of shocks could play a role in the formation of relatively wide regions of atomic gas, which could also be cooled through fine-structure atomic lines (see Hollenbach & McKee 1989).

In this paper we analyze the results of our ISO data (that in some cases have been improved with data found in the ISO data archive or in Liu et al. 2001), and their comparison with models in order to infer the origin of the emission of the low-excitation atomic gas. In Castro-Carrizo et al. (2001) and Fong et al. (2001) a detailed description of the data, the comparison with models, and the calculation of the masses are found, for O-rich and C-rich sources respectively.

2. ISO OBSERVATIONS

Our sample is composed of 24 sources, mostly PPNe but also including a few planetary nebulae and AGB stars for comparison. The observed O-rich sources are: OH 26.5+0.6, Mira, Betelgeuse, R Sct, AFGL 2343, HD 161796, 89 Her, M 1-92, M 2-9, Hb 12, Mz-3, and NGC 6302. The C-rich sources are: IRC +10216, IRAS 15194-5115, LP And, IRAS 22272+5435, AC Her, SAO 163075, AFGL 2688, Red Rectangle, IRAS 21282+5050, AFGL 618, NGC 6720, and NGC 7027. We also observed off-source points to determine if interstellar medium (ISM) contribution exists, and in that case to estimate the emission that comes from the nebula.

In order to study the low-excitation atomic gas we observed the following fine-structure atomic lines: [O I] (63.2 μm , 145.5 μm), [C II] (157.7 μm), [N II] (121.9 μm), [Si I] (68.5 μm , 129.7 μm), [Si II] (34.8 μm), [S I] (25.2 μm), [Fe I]

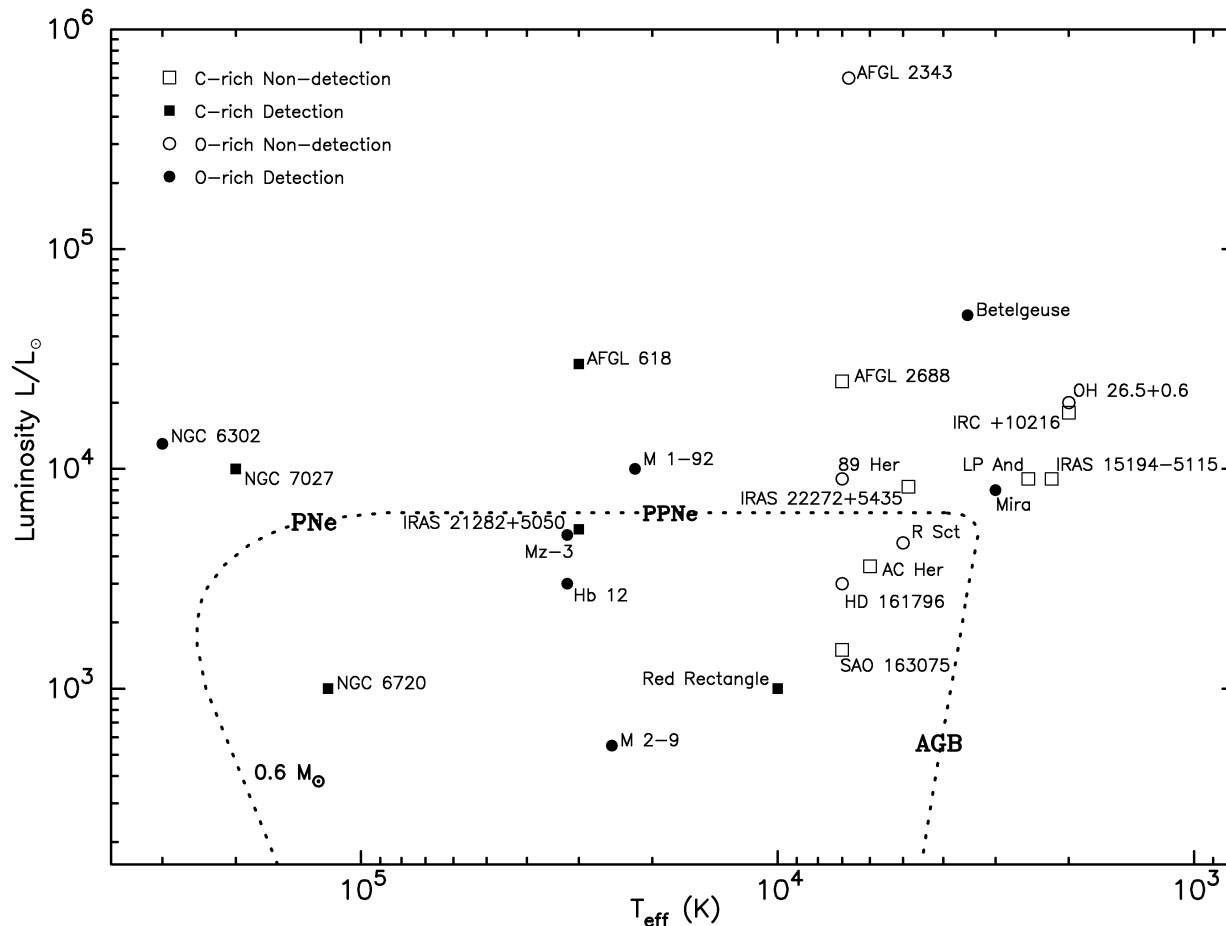


Figure 1. Distribution in the H-R diagram of the observed sources.

($24.0 \mu\text{m}$, $34.7 \mu\text{m}$) and [Fe II] ($26.0 \mu\text{m}$, $35.3 \mu\text{m}$). We used both ISO spectrometers, LWS ($43\text{--}196.7 \mu\text{m}$) and SWS ($2.4\text{--}45 \mu\text{m}$), according to different observational modes, grating and Fabry-Perot (FP).

Only the FP observations allowed obtaining enough spectral resolution to study the kinematics of the emitting sources, but due to the poor sensitivity of the FP modes the analysis becomes very difficult. On the other hand, the more sensitive grating modes do allow us to get reliable line fluxes for the detected sources. (All our LWS-FP lines have been also observed by grating modes.) The typical rms obtained with the LWS/SWS grating is $\sim 0.1\text{--}1/1\text{--}10 \cdot 10^{-12} \text{ erg cm}^{-2}\text{s}^{-1}\mu\text{m}^{-1}$. The peak intensity of the most intense detected lines is $\sim 10^{-8} \text{ erg cm}^{-2}\text{s}^{-1}\mu\text{m}^{-1}$ for PNe, and $\sim 10^{-9}\text{--}10^{-10} \text{ erg cm}^{-2}\text{s}^{-1}\mu\text{m}^{-1}$ for PPNe.

In Figure 1 we represent all the observed nebulae in an H-R diagram, showing the temperatures and the luminosities of the central stars. The sources are marked with filled symbols when some of the observed atomic lines was

detected. For a subsequent interpretation of the data it is also important to note that the number of detected lines and their intensities increase for sources surrounding hotter central star.

We have also found that the ratio of the most intense lines, [O I] $63 \mu\text{m}$ /[C II] $158 \mu\text{m}$, is very different when emission comes from sources or from ISM contamination, being < 1 when emission comes from ISM and $>$ or $\gg 1$ when it comes from the nebulae. This fact has helped us to infer the origin of the detections in those few cases for which we did not observed off-source points.

3. INTERPRETATION OF THE DATA

3.1. DEPENDENCE ON STELLAR PARAMETERS

One of the main results of this work is obtained by comparison of the observed data with the stellar parameters, i.e., with the evolutionary stage of the sources. Figure 1 shows that only nebulae surrounding stars hotter than $\sim 10000 \text{ K}$

are detected, and we have mentioned that as the T_{eff} increases above 10000K the line emission is more intense and the number of lines detected is higher. The only exceptions are the detection of several lines in Betelgeuse and the probable detection [O I] 63 μm in Mira. Betelgeuse is a red supergiant star which shows a well studied UV excess, probably due to a very hot chromosphere, and Mira has a hotter binary companion. Moreover, this dependence on the stellar temperature is strengthened by the fact that among emitters and non-emitters there are very similar objects, from the point of view of their morphology, presence of shocks, chemistry and total nebular mass, but with different low-excitation atomic emission and different T_{eff} of the central star (see for example the case of AFGL 2688 and AFGL 618). It is also noticeable the lack of emission from the very massive molecular nebulae AFGL 2343 and HD 161796.

We interpret this result as showing that the total mass of the low-excitation atomic gas strongly depends on the temperature of the central star. This suggests that the emitting region is a PDR caused by stellar UV photons, not due to shocks nor ISM photons.

3.2. LINE PROFILE ANALYSIS; KINEMATICS

Fabry-Perot profiles were obtained of M 2–9, IRAS 21282, AFGL 618, Hb 12, Mz-3, Hb 12, NGC 6720, NGC 7027 and NGC 6302. After *deconvolution* of the instrumental profile, we have analyzed the spectral profiles of those detected lines, in order to study the kinematics of the emitting regions. However, this analysis becomes quite uncertain for our sources due to the mentioned poor sensitivity of the FP observations.

The main conclusion is that the widths of our *deconvolved* FP profiles are in general comparable to those of low-velocity CO emission ($\lesssim 40 \text{ km s}^{-1}$). Note that much higher velocities would be expected from shocked regions. This suggests that atomic line emission mostly arises from PDRs.

However, in two particular cases, M 2–9 and AFGL 618, part of the emission probably comes from shocks, since their profiles seem to show high-velocity expanding features (with a poor signal to noise ratio). For example, whereas from the profile of the [O I] 63 μm line from a young PN, NGC 7027, we have found an expansion velocity of $\sim 20 \text{ km s}^{-1}$, to fit the profile of that emission coming from AFGL 618 we have needed to assume that there exists a gas component expanding at $\sim 70 \text{ km s}^{-1}$. Higher sensitivity and spectral resolution are needed to confirm those shocked components, and in that case to determine the portion of mass accelerated. Also for our other sources we expect to find minor atomic high-velocity components with a more sensitive instrument.

3.3. PDR MODELS

Our data have been compared with predictions of PDR models. For the O-rich sources we used the last improved version of the models of Tielens & Hollenbach (1985), published by van den Ancker (1999). For the C-rich sources new models have been developed by Latter & Tielens (2001) taking into account the complex and different treatment of the chemistry, what necessarily changes the physical conditions of the gas. The models solve the chemical and the thermal balance in the gas, and predict the emission from these regions primarily as a function of the incident far-ultraviolet flux (G) and of the density (n) in that region. Note the importance of the parameter G , that represents the radiation field relevant for the photoelectric effect, and which is the main PDR heater.

The comparison of our data with models is quite satisfactory, since the physical parameters required to explain the data are quite compatible for the different lines of each source. In particular, the densities obtained from this analysis mostly range from 10^4 to 10^6 particles per cm^{-3} . The main disagreement is that our PDR predictions do not account for the strong contrast found between the atomic emission of the nebulae around stars with more or less than $\sim 10000 \text{ K}$. The reason could be in the initial assumptions of the models. In the way we are using the theory, the only parameter of the models that depends on T_{eff} is G . However, note that the number of photons able to dissociate CO, which have between 6 and 11 eV, decreases considerably for the coolest stars, and that the effective temperature assumed by the models is 30000 K. This fact can lead to an overestimation of the dissociation capacity for the coolest sources. In addition, the model assumption of chemical and physical equilibrium could be not satisfied for the coolest sources, and in that case this could contribute to overestimating the emission of those objects.

3.4. SHOCK MODELS

The shock theory used, for both J- and C-type shocks, predicts the intensity emitted through FIR lines from the shock velocity and the pre-shock density. Those theoretical curves have been adapted from van den Ancker (1999) for all the observed lines. The comparison of our data with this theory of atomic line emission from shock excited regions is less satisfactory than it was with the PDR theory. Different shock parameters, velocities and densities, are needed to reproduce the intensities observed for the different lines of each source. In the case of J-type shocks, the observed [C II] intensities are too large for all models taken into account, even those with very high shock velocity ($\sim 100 \text{ km s}^{-1}$). For C-type shocks, models cannot explain the observed ionized atoms. Therefore, this analysis also suggests that the observed emission is not mainly caused by shocks.

4. ATOMIC MASS CALCULATIONS

Probably the best tracer of this low-excitation atomic regions is [C II] 158 μm , thanks to the high abundance of C⁺ in most of the PDR and to its easy analysis. Note that C⁺ appears almost at the same time that CO is photodissociated, being the C⁰ region very thin for the O-rich case, or coincident with the CO region (from the dissociation of other molecules) for the C-rich case. Moreover, C⁺ is soon photoionized in the H⁺ region.

The analysis of the [C II] 158 μm line is easy because the following conditions are fulfilled. First, the total mass is independent of the excitation conditions, density and gas temperature, because for the values expected the population of the involved levels becomes constant. Secondly, we have checked that this emission in our cases is optically thin.

The mass of the low-excitation atomic gas is then given by the equation 1,

$$M(M_{\odot}) = 7.010^6 F_{[\text{C II}]} (\text{erg cm}^{-2} \text{s}^{-1}) D(\text{kpc})^2 / \chi_{\text{C}} \quad (1)$$

where $F_{[\text{C II}]}$ is the flux of the [C II] 158 μm line, D is the distance to the source and χ_{C} is the abundance of C. For our calculations for O-rich sources, we have taken $\chi_{\text{C}} = 3 \cdot 10^{-4}$, and for each C-rich source we have taken the best value found in the bibliography. When [C II] 158 μm was not detected, we have estimated an upper limit.

For the few cases in which we expect very low densities ($n \lesssim 10^3 \text{ cm}^{-3}$) we must multiply this mass calculation by a correction factor (> 1) that takes into account the dependence of the mass on the excitation conditions. Only for NGC 6720 and Hb 12, it has been necessary to include this correction factor, with the values 2.5 and 1.5 respectively.

In Table 4 we show our calculations for the low-excitation atomic gas (M_{atom}) and, by comparison, the mass of the molecular and the ionized gas found in the bibliography, considering the same distance values. In the last column we note the chemical type of each source and the presence of ISM contamination.

From the mass calculations we see that the atomic region increases when the sources evolve towards planetary nebulae, because of photodissociation. However, it is noticeable that the mass of the low-excitation atomic gas is relatively important for the most evolved sources, and even the most important component for Hb 12 and NGC 6302, becoming $\sim 1 M_{\odot}$. Note also the particular cases of M 2-9 and 89 Her, for which a global deficiency of mass has been found. Another point to note is that the amount of atomic gas found does not seem to be related to the chemistry of the nebula.

ACKNOWLEDGEMENTS

Castro-Carrizo and Bujarrabal have been partially supported by the Spanish CYCIT, the European Commission and the PNIÉ under grants PB96-104, 1FD1997-1442 and ESP99-1291-E. Fong and Meixner have been supported by NASA JPL 961504, NASA NAG 5-3350 and NSF AST-97-33697. Latter

source	M_{atom} (M_{\odot})	M_{mol} (M_{\odot})	M_{ion} (M_{\odot})	
Mira	$< 2 \cdot 10^{-4}$	$1.5 \cdot 10^{-4}$		O
Betelgeuse	$2 \cdot 10^{-4}$	$4 \cdot 10^{-4}$		O
IRAS 22272+5435	< 0.01	0.56		C, <i>ISM</i>
R Sct	< 0.002	0.002		O, <i>ISM</i>
AC Her	< 0.01	$1.1 \cdot 10^{-4}$		C
AFGL 2343	< 1	4.8		O, <i>ISM</i>
HD 161796	< 0.05	0.68		O
SAO 163075	< 0.001	0.03		C
AFGL 2688	< 0.02	0.6		C
89 Her	< 0.005	0.0043		O
Red Rectangle	< 0.002	$2.5 \cdot 10^{-5}$		C, <i>ISM?</i>
M 1-92	< 0.2	0.9		O, <i>ISM</i>
M 2-9	0.04	0.005	0.004	O
IRAS 21282+5050	0.1	2.7	0.008	C
AFGL 618	0.01	1.6	$4 \cdot 10^{-4}$	C, <i>ISM?</i>
Hb 12	0.3	< 0.001	0.015	O
Mz-3	< 0.7	0.5	0.2	O, <i>ISM</i>
NGC 6720	0.18	0.34	0.2	C
NGC 7027	0.2	1.4	0.04	C
NGC 6302	1.3	0.1	0.2	O

Table 1. Low-excitation atomic gas masses derived from [C II] line flux. Mass estimates of the molecular region from ¹²CO emission and of the ionized gas are given by comparison. Chemical information and the possible contribution of the ISM are given in the last column.

and Tielens acknowledge additional support from NASA grant 399-20-61 from the Long Term Space Astrophysics Program.

REFERENCES

- Castro-Carrizo A., Bujarrabal V., Fong D., Meixner M., Tielens A.G.G.M., Latter W.B. & Barlow M.J., A&A, in press.
 Fong D., Meixner M., Castro-Carrizo A., Bujarrabal V., Latter W., Tielens A.G.G.M., Kelly D. & Sutton E., A&A, in press.
 Hollenbach D. & McKee C.F., 1989, ApJ 342, 306
 Latter W.B. & Tielens A.G.G.M., in preparation.
 Liu X.-W., Barlow M.J., Cohen M., Danziger I.J., Luo S.-G. et al., 2001, MNRAS, in press.
 Tielens A.G.G.M. & Hollenbach D., 1985, ApJ 291, 722
 van den Ancker M.E., 1999, Ph.D. Thesis.